Analysis of bulk heterojunction organic solar cell blends by solid-state NMR relaxometry and sensitive external quantum efficiency – Impact of polymer side chain variation on nanoscale morphology

Supplementary material

DEVISSCHER, Dries; REEKMANS, Gunter; KESTERS, Jurgen; VERSTAPPEN, Pieter; Benduhn, Johannes; Van den Brande, Niko; LUTSEN, Laurence; MANCA, Jean; VANDERZANDE, Dirk; VANDEWAL, Koen; ADRIAENSENS, Peter & MAES, Wouter (2019) Analysis of bulk heterojunction organic solar cell blends by solid-state NMR relaxometry and sensitive external quantum efficiency – Impact of polymer side chain variation on nanoscale morphology. In: ORGANIC ELECTRONICS, 74, p. 309-314.

DOI: 10.1016/j.orgel.2019.06.046
Handle: http://hdl.handle.net/1942/29634

Supplementary Data

Analysis of Bulk Heterojunction Organic Solar Cell Blends by Solid-State NMR Relaxometry and Sensitive External Quantum Efficiency – Impact of Polymer Side Chain Variation on Nanoscale Morphology

Dries Devisscher,[1,2] Gunter Reekmans,[1,2] Jurgen Kesters,[1,2] Pieter Verstappen,[1,2] Johannes Benduhn,[3] Niko Van den Brande,[4] Laurence Lutsen,[2] Jean Manca,[5] Dirk Vanderzande,[1,2] Koen Vandewal,[1,2] Peter Adriaensens[1,2] and Wouter Maes[1,2,]*

[1] UHasselt – Hasselt University, Institute for Materials Research (IMO-IMOMEC), Agoralaan 1, 3590 Diepenbeek, Belgium

[2] IMOMEC Division, IMEC, Wetenschapspark 1, 3590 Diepenbeek, Belgium

[3] Institut für Angewandte Photophysik, Technische Universität Dresden, Germany

[4] Vrije Universiteit Brussel, Pleinlaan 2, 1050 Brussels, Belgium

[5] UHasselt – Hasselt University, X-LAB, Agoralaan 1, 3590 Diepenbeek, Belgium

Table of Contents

1. General Experimental Methods

All reagents and chemicals were obtained from commercial sources and used without further purification. Solvents were dried on a solvent purification system (MBraun, MB-SPS-800) equipped with alumina columns. $PC_{71}BM$ was obtained from Solenne BV and used without purification. Solution NMR measurements were performed in $CDCl_3$ on a 400 MHz instrument (Varian). The chemical shifts (δ, in ppm) were determined relative to the residual $CHCl_3$ (7.26 ppm) proton signal. Polymer weight distributions were estimated through gel permeation chromatography (GPC) on an Agilent Technologies PL-GPC 220 high temperature chromatograph with PL-GEL 10 mm MIXED-C column, calibrated with polystyrene internal standards and with *o*-dichlorobenzene at 140 °C as the eluent. Prior to the measurements, the samples were stirred at 140 °C until the polymers dissolved completely. UV-Vis absorption spectroscopy measurements were performed on a VARIAN Cary 500 UV-Vis-NIR spectrophotometer at a scan rate of 600 nm min^{-1}. The films for the UV-Vis measurements were prepared by drop casting a solution of the polymer in chlorobenzene on a quartz substrate. The solid-state UV-Vis spectra were used to estimate the optical gaps (from the wavelength at the intersection of the tangent line drawn at the low energy side of the absorption spectrum with the x-axis: E_g (eV) = 1240/(wavelength in nm)). Electrochemical measurements (cyclic voltammetry, CV) were performed with an Eco Chemie Autolab PGSTAT 30 potentiostat/galvanostat using a three-electrode microcell with a platinum working electrode, a platinum counter electrode and a $Ag/AgNO_3$ reference electrode (Ag wire dipped in a solution of 0.01 M $AgNO_3$ and 0.1 M NBu_4PF_6 in anhydrous acetonitrile). The reference electrode was calibrated against ferrocene/ferrocenium as an external standard. Samples were prepared by dip-coating the platinum working electrode in the respective polymer solutions (also used for the solid-state UV-Vis measurements). The CV measurements were done on the resulting films with 0.1 M NBu_4PF_6 in anhydrous acetonitrile as electrolyte solution. To prevent air from entering the system, the experiments were carried out under a curtain of argon. Cyclic voltammograms were recorded at a scan rate of 100 mV s^{-1}. For the conversion of V to eV, the onset potentials of the first oxidation/reduction peaks were used and referenced to ferrocene/ferrocenium, which has an ionization potential of −4.98 eV *vs.* vacuum. This correction factor is based on a value of 0.31 eV for Fc/Fc^+ *vs.* SCE[1] and a value of 4.68 eV for SCE *vs.* vacuum[2]: $E_{HOMO/LUMO}$ (eV) = −4.98 − $E_{onset\ ox/red}^{Ag/AgNO3}$ (V) + $E_{onset\ Fc/Fc+}^{Ag/AgNO3}$ (V). The reported values are the means of the first four redox cycles. Rapid heat-cool calorimetry (RHC) experiments were performed on prototype equipment developed by TA Instruments, equipped with liquid nitrogen cooling and specifically designed for operation at high scanning rates. RHC measurements were performed at 500 K min^{-1} (after cooling at 20 K min^{-1}) using dedicated aluminum crucibles filled with samples of 200–250 µg, using helium (10 mL min^{-1}) as a purge gas.

2. Synthesis Procedures

2.1. Monomer Synthesis

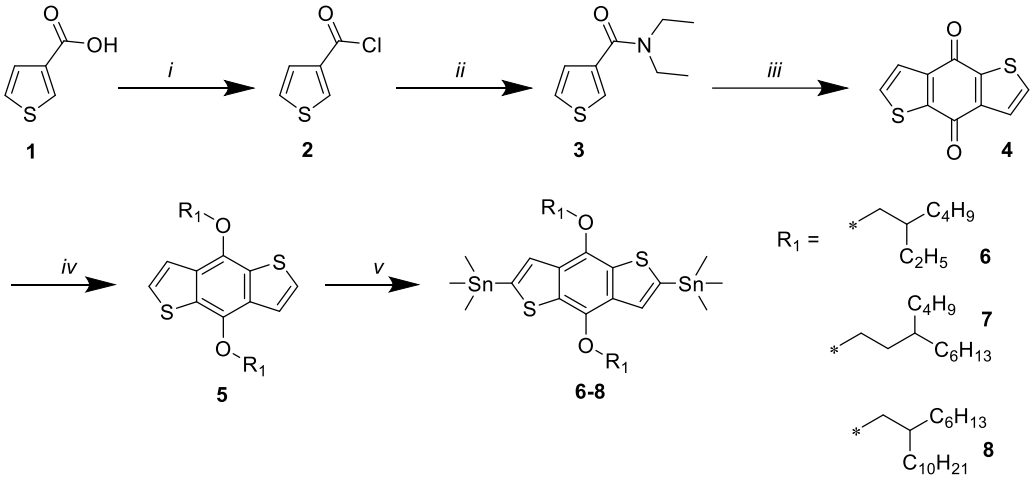

Scheme S1: Synthesis of bis(stannyl)-BDT monomers **6**–**8**: i) thionyl chloride, 2 h at 80 °C (95%); ii) diethylamine, CH_2Cl_2, 2 h at 0 °C (90%); iii) *n*-BuLi, THF, 5 h at 0 °C (78%); iv) metallic zinc, NaOH, tetra-*n*-butylammonium bromide, alkyl bromide, water, 5 h at reflux temperature (73-85%); v) *n*-BuLi, trimethyltin chloride, 1.5 h at −78 °C, overnight at RT (84-89%).

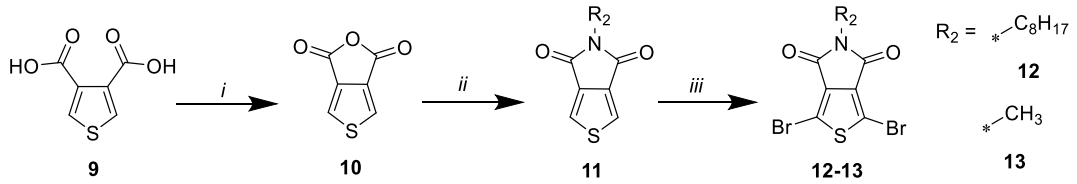

Scheme S2: Synthesis of dibromo-TPD monomers **12** and **13**: i) acetic anhydride, 4 h at reflux temperature (87%); ii) thionyl chloride, alkylamine, THF, 7 h at 50 °C (79-86%); iii) Br_2, AcOH, 5 h at reflux temperature (73-79%).

2.2. Polymer Synthesis

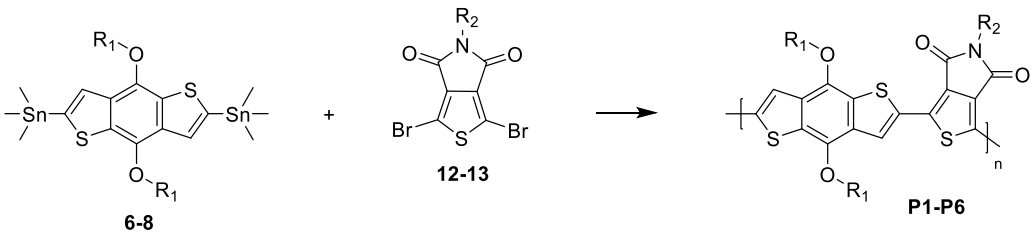

Scheme S3: P(BDT-*alt*-TPD) copolymer synthesis by Stille cross-coupling. All polymerizations were performed with 3 mol% Pd_2dba_3 and 12 mol% P(*o*-tol)$_3$ in chlorobenzene at 110 °C for 16 h.

P1. (4,8-Bis(2-ethylhexyloxy)benzo[1,2-*b*:4,5-*b*']dithiophene-2,6-diyl)bis(trimethylstannane) (**6**) (130 mg, 0.168 mmol) and 1,3-dibromo-5-octyl-4*H*-thieno[3,4-*c*]pyrrole-4,6(5*H*)-dione (**12**) (71 mg, 0.168 mmol), $Pd_2(dba)_3$ (4.6 mg, 0.005 mmol) and tri(*o*-tolyl)phosphine (6.1 mg, 0.020 mmol) were added to a dried schlenk tube. Nitrogen purged chlorobenzene (3 mL) was added and the mixture was then stirred overnight at 110 °C under nitrogen atmosphere. After cooling to room temperature, the mixture was transferred to a round-bottom flask and chloroform (100 mL) was added, together with water (100 mL) containing sodium diethyldithiocarbamate (1.0 g). This mixture was then stirred for 1 h at 60 °C under nitrogen atmosphere. The organic layer was subsequently collected and partially evaporated under lowered pressure. The polymer was then precipitated in methanol, filtered off and transferred to a Soxhlet thimble. Soxhlet extractions with methanol, acetone, *n*-hexane and dichloromethane were performed. The polymer was then collected with chlorobenzene and again precipitated in methanol, after which the final polymer sample was collected by filtration (98 mg, 82%).

P2. The polymerization procedure was performed according to the protocol outlined for **P1**. (4,8-Bis(2-ethylhexyloxy)benzo[1,2-*b*:4,5-*b*']dithiophene-2,6-diyl)bis(trimethylstannane) (**6**) (85 mg, 0.110 mmol), (4,8-bis(3-butylnonyloxy)benzo[1,2-*b*:4,5-*b*']dithiophene-2,6-diyl)bis(trimethylstannane) (**7**) (110 mg, 0.110 mmol) and 1,3-dibromo-5-methyl-4*H*-thieno[3,4-*c*]pyrrole-4,6(5*H*)-dione (**13**) (71.2 mg, 0.220 mmol) were polymerized in nitrogen purged chlorobenzene (3 mL) in a dried schlenk tube with $Pd_2(dba)_3$ (6.0 mg, 0.007 mmol) and tri(*o*-tolyl)phosphine (8 mg, 0.026 mmol). Soxhlet extractions were performed with methanol, acetone, *n*-hexane, dichloromethane and chloroform. The chloroform fraction was added to methanol, after which the final polymer sample was collected by filtration (116 mg, 76%).

P3. The polymerization procedure was performed according to the protocol outlined for **P1**. (4,8-Bis(3-butylnonyloxy)benzo[1,2-*b*:4,5-*b*']dithiophene-2,6-diyl)bis(trimethylstannane) (**7**) (100 mg, 0.110 mmol) and 1,3-dibromo-5-methyl-4*H*-thieno[3,4-*c*]pyrrole-4,6(5*H*)-dione (**13**) (35.6 mg, 0.110 mmol) were polymerized in nitrogen purged chlorobenzene (3 mL) in a dried schlenk tube with $Pd_2(dba)_3$ (3.0 mg, 0.003 mmol) and tri(*o*-tolyl)phosphine (4.0 mg, 0.013 mmol). Soxhlet extractions were performed with methanol, acetone, *n*-hexane, dichloromethane and chloroform. The chloroform fraction was added to methanol, after which the final polymer sample was collected by filtration (60 mg, 73%).

P4. The polymerization procedure was performed according to the protocol outlined for **P1**. (4,8-Bis(2-octyldodecyloxy)benzo[1,2-*b*:4,5-*b*']dithiophene-2,6-diyl)bis(trimethylstannane) (**8**) (169 mg, 0.154 mmol) and 1,3-dibromo-5-methyl-4*H*-thieno[3,4-*c*]pyrrole-4,6(5*H*)-dione (**13**) (50.2 mg, 0.154 mmol) were polymerized in nitrogen purged chlorobenzene (3 mL) in a dried schlenk tube with $Pd_2(dba)_3$ (4.2 mg, 0.005 mmol) and tri(*o*-tolyl)phosphine (5.6 mg, 0.019 mmol). Soxhlet extractions were performed with methanol, acetone, and *n*-hexane. The *n*-hexane fraction was added to methanol, after which the final polymer sample was collected by filtration (90 mg, 62%).

P5. The polymerization procedure was performed according to the protocol outlined for **P1**. (4,8-Bis(2-ethylhexyloxy)benzo[1,2-*b*:4,5-*b*']dithiophene-2,6-diyl)bis(trimethylstannane) (**6**) (100 mg, 0.129 mmol), 1,3-dibromo-5-octyl-4*H*-thieno[3,4-*c*]pyrrole-4,6(5*H*)-dione (**12**) (49.3 mg, 0.117 mmol) and 1,3-dibromo-5-methyl-4*H*-thieno[3,4-*c*]pyrrole-4,6(5*H*)-dione (**13**) (4.2 mg, 0.013 mmol) were polymerized in nitrogen purged chlorobenzene (3 mL) in a dried schlenk tube with $Pd_2(dba)_3$ (3.6 mg, 0.004 mmol) and tri(*o*-tolyl)phosphine (4.7 mg, 0.016 mmol). Soxhlet extractions were performed with methanol, acetone, *n*-hexane, dichloromethane and chloroform. The chloroform fraction was added to methanol, after which the final polymer sample was collected by filtration (80 mg, 88%).

P6. The polymerization procedure was performed according to the protocol outlined for **P1**. (4,8-Bis(2-ethylhexyloxy)benzo[1,2-*b*:4,5-*b*']dithiophene-2,6-diyl)bis(trimethylstannane) (**6**) (100 mg, 0.129 mmol), 1,3-dibromo-5-octyl-4*H*-thieno[3,4-*c*]pyrrole-4,6(5*H*)-dione (**12**) (43.8 mg, 0.104 mmol) and 1,3-dibromo-5-methyl-4*H*-thieno[3,4-*c*]pyrrole-4,6(5*H*)-dione (**13**) (8.4 mg, 0.026 mmol) were polymerized in nitrogen purged chlorobenzene (3 mL) in a dried schlenk tube with $Pd_2(dba)_3$ (3.6 mg, 0.004 mmol) and tri(*o*-tolyl)phosphine (4.7 mg, 0.016 mmol). Soxhlet extractions were performed with methanol, acetone, *n*-hexane, dichloromethane and chloroform. The chloroform fraction was added to methanol, after which the final polymer sample was collected by filtration (76 mg, 85%).

3. Gel Permeation Chromatography

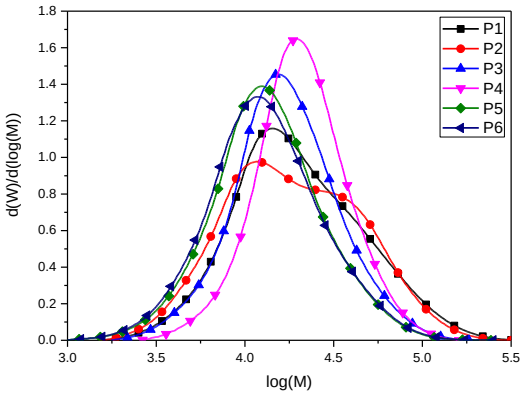

Figure S1: Gel permeation chromatograms for the PBDTTPD polymer series (chlorobenzene, 140 °C).

Table S1: Number-average molar masses and dispersities for the PBDTTPD polymers as determined by high-temperature gel permeation chromatography.

	M_n (kg mol^{-1})	$Đ$
P1	14.8	2.03
P2	13.5	2.12
P3	13.8	1.59
P4	17.6	1.43
P5	10.6	1.69
P6	10.2	1.73

4. Cyclic Voltammetry Data

Table S2: Electrochemical properties of the PBDTTPD polymer series.

	E^{ox}_{onset} (V)	HOMO (eV)	E^{red}_{onset} (V)	LUMO (eV)	$E_{g,EC}$ (eV)	$E_{g,opt}$ (eV)
P1	0.73	-5.63	-1.69	-3.21	2.42	1.86
P2	0.61	-5.52	-1.69	-3.22	2.30	1.85
P3	0.70	-5.60	-1.70	-3.21	2.40	1.83
P4	0.81	-5.71	-1.68	-3.22	2.50	1.85
P5	0.50	-5.41	-1.66	-3.24	2.17	1.85
P6	0.51	-5.51	-1.68	-3.22	2.30	1.82

5. UV-Vis Absorption Spectra

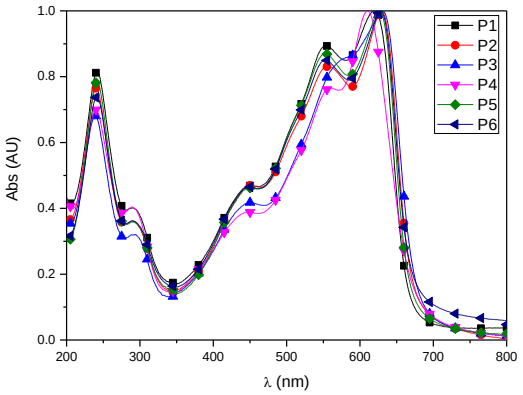

Figure S2: Normalized UV-Vis absorption spectra for the PBDTTPD polymers in thin film.

6. Photovoltaic Device Fabrication and Characterization

Bulk heterojunction organic solar cells were fabricated using the standard architecture glass/ITO/PEDOT:PSS/active layer/Ca/Al. Prior to device processing, the indium-tin oxide (ITO) coated substrates (100 nm, Kintec, sheet resistivity 20 Ω sq^{-1}) were subjected to a standard cleaning procedure using soap, demineralized water, acetone and isopropanol, followed by a UV/O_3 treatment for 15 min. PEDOT:PSS [poly(3,4-ethylenedioxythiophene):poly(styrenesulfonic acid), Heraeus Clevios] was deposited by spin-coating and the layer was annealed at 130 °C for 15 min in ambient air, aiming at a layer thickness of ~30 nm. Further processing was in all cases performed under nitrogen atmosphere inside a glove box (<1 ppm O_2/H_2O). The photoactive layer solutions were prepared by dissolving the donor polymer and acceptor fullerene with a donor:acceptor ratio of 1:1.5 (wt/wt) in different solvents at different concentrations (cfr. Table S3). The solutions were stirred in a sealed vial overnight at 80 °C. The active layer was deposited on top of the PEDOT:PSS layer by means of spin-coating at room temperature with an optimal layer thickness of 80 to 100 nm. To ensure proper removal of the additive (whenever used) from the photoactive layer, the samples were placed in a vacuum chamber with a pressure of 5 x 10^{-7} mbar for 1 h. In a final step, the top electrodes Ca and Al were deposited by vacuum deposition with layer thicknesses of 30 and 80 nm, respectively. Complete solar cell devices with an active area of 3 mm^2 were obtained.

The *I-V* characteristics of all photovoltaic devices were evaluated under AM1.5G solar illumination (100 mW cm^{-2}) using a Newport class A solar simulator (model 91195A) calibrated with a silicon solar cell. EQE measurements were performed with a Newport Apex illuminator (100 W Xenon lamp, 6257) as light source, a Newport Cornerstone 130° monochromator and a Stanford SR830 lock-in amplifier for the current measurements. A silicon FDS100-CAL photodiode was employed as a reference cell.

For the sEQE measurements, the light of a quartz halogen lamp (50 W) was chopped at 140 Hz and coupled into a monochromator (Newport Cornerstone 260 1/4m, USA). The resulting monochromatic light was focused onto the solar cell and it's short-circuit current was pre-amplified before it was analysed with a lock-in amplifier (Signal Recovery 7280 DSP, USA). The time constant of the lock-in amplifier was chosen to be 1s and the amplification of the pre-amplifier was increased to resolve low photocurrents. The EQE is determined by dividing the photocurrent of the photovoltaic device by the flux of incoming photons, which was measured using a calibrated Si and InGaAs photodiode.

AFM experiments were performed with a JPK NanoWizard 3 AFM (JPK Instruments AG, Berlin, Germany) using AC mode in air. Silicon ACTA-50 tips from AppNano with a cantilever length of ~125 mm, a spring constant of ~40 N m^{-1} and a resonance frequency of ~300 kHz were used. The scan angle, set point height, gain values and scan rate were adjusted according to the calibration of the AFM tip.

Table S3: Solar cell device optimization overview.

	Processing solvent[a]	Polymer concentration (mg mL^{-1})	V_{OC}[b] (V)	J_{SC}[b] (mA cm^{-2})	FF[b]	PCE[b] (%)	Best PCE (%)
P1[c]	CB + 5% CN	8	0.93	10.13	0.66	6.17	6.42
P2	CB + 5% CN	8	0.84	9.87	0.67	5.57	5.88
P2	ODCB	8	0.84	8.57	0.64	4.64	4.88
P3	CF	6	0.68	3.77	0.56	1.44	1.52
P3	CF + 5% ODCB	6	0.76	7.58	0.57	3.29	3.38
P3	CB	8	0.60	4.52	0.55	1.50	1.53
P3	CB + 5% CN	8	0.73	5.55	0.54	2.19	2.32
P3	ODCB	8	0.68	6.76	0.57	2.63	2.73
P3	ODCB + 5% CN	8	0.72	4.95	0.56	1.98	2.06
P5	CF	6	0.93	4.37	0.59	2.38	2.49
P5	CF + 5% ODCB	6	0.89	8.98	0.54	4.31	4.66
P5	CB	8	0.89	6.36	0.59	3.34	3.81
P5	CB + 5% CN	8	0.88	9.71	0.58	4.95	5.11
P6	CF	6	0.93	4.70	0.56	2.45	2.60
P6	CF + 5% ODCB	6	0.89	9.79	0.51	4.45	4.76
P6	CB	8	0.89	7.16	0.63	4.03	4.20
P6	CB + 5% CN	8	0.85	8.39	0.44	3.16	3.31

[a] Chlorobenzene (CB), chloronaphthalene (CN), orthodichlorobenzene (ODCB), chloroform (CF). [b] Averaged values over 4 devices. [c] Processing conditions based on literature.[3]

7. External Quantum Efficiency

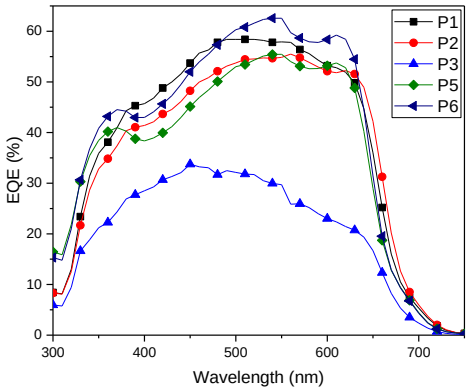

Figure S3: EQE spectra for average performing solar cell devices (J_{EQE} values (mA cm^{-2}) for **P1**: 9.48, **P2**: 9.17, **P3**: 4.88, **P5**: 8.69, **P6**: 9.68).

8. Differential Scanning Calorimetry

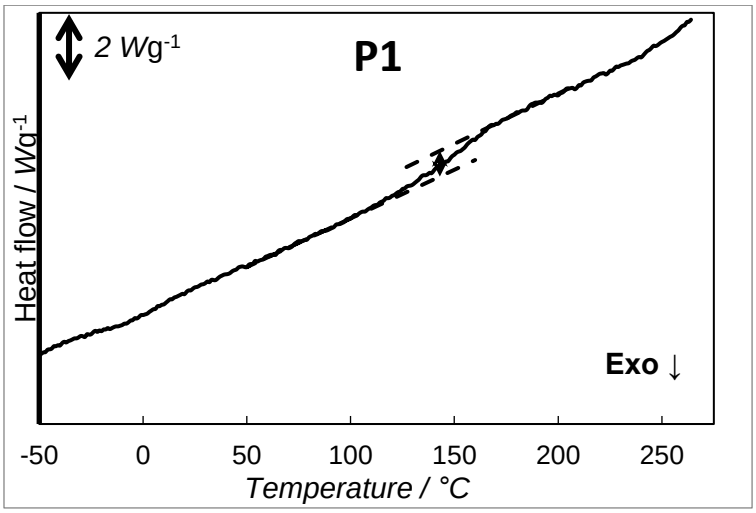

Figure S4: RHC thermogram for the reference polymer **P1** (2nd heating curve). The presence of a glass transition temperature at 143 °C and the absence of a melting peak (within the temperature window studied, i.e. up to 300 °C) suggest an amorphous nature for this polymer.

9. Proton Wideline Solid-State NMR Relaxometry

9.1. Sample Preparation

The proton wideline solid-state NMR samples were prepared by dissolving 30 mg of the polymer:fullerene blend (with a donor:acceptor ratio of 1:1.5; wt/wt) in the respective solvent and at the concentration that provided the best solar cell result for each donor polymer (cfr. Table S3). The solutions were then stirred in a sealed vial overnight at 80 °C. The photoactive layer blend was drop-casted on a glass substrate that was heated at a constant temperature of 90 °C. After a drying time of 2 min, the substrate was removed from the heating source and cooled to ambient temperature. The blend was then removed mechanically from the substrate using a razor blade. The solid was subsequently dried under vacuum overnight to remove any residual solvent.

9.2 Experimental Details

Proton wideline solid-state NMR relaxation measurements were carried out at ambient temperature on a Varian/Agilent Inova 400 spectrometer in a dedicated wideline probe equipped with a 5 mm coil using the solid echo method ($90°_{x'}$ - t_{se} - $90°_{y'}$ - t_{se} - acquire) to overcome the effect of the dead-time of the receiver. The 90° pulse length t_{90} was 1.3 µs and spectra were recorded with a spectral width of 2 MHz (0.5 µs dwell time), allowing an accurate determination of the echo maximum. Samples were placed in 5 mm glass tubes closed tightly with teflon stoppers.
The T_{1H} relaxation decay times (spin-lattice relaxation in the lab frame) were measured by placing an inversion recovery filter in front of the solid echo part ($180°_{x'}$ - t - $90°_{x'}$ - t_{se} - $90°_{y'}$ - t_{se} - acquire). The integrated proton signal intensity was analyzed bi-exponentially for $PC_{71}BM$ and mono-exponentially for the polymers and polymer blends as a function of the variable inversion time t according to:

$$I(t) = I_o^S.(1 - 2.\exp(-t/T_{1H}^S)) + I_o^L.(1 - 2.\exp(-t/T_{1H}^L)) + c^{te} \qquad \textbf{(Eq. S1)}$$

'S' and 'L' refer here to the fractions with short and long decay time, respectively.

The $T_{1\rho H}$ relaxation decay times (spin-lattice relaxation in the rotating frame) were measured by applying a spin-lock field (45 kHz) of variable duration, t_{SL}, after the initial 90°$_{x'}$ pulse in the solid echo pulse sequence (90°$_{x'}$-t_{SL}-t_{se}-90°$_{y'}$- t_{se}-acquire). The integrated proton signal intensity was analyzed bi-exponentially as a function of the variable duration of the spin-lock field t_{SL} according to the equation:

$$I(t) = I_o^S.\exp(-t/T_{1\rho H}^S) + I_o^L.\exp(-t/T_{1\rho H}^L) + c^{te} \qquad \textbf{(Eq. S2)}$$

'S' and 'L' again refer to the fractions with short and long decay time, respectively.
All experimental data were analyzed using a non-linear least-squares fit (Levenberg-Marquardt algorithm). A preparation delay of 15 s was always used between successive accumulations to obtain quantitative results.

9.3. Correlation Plot

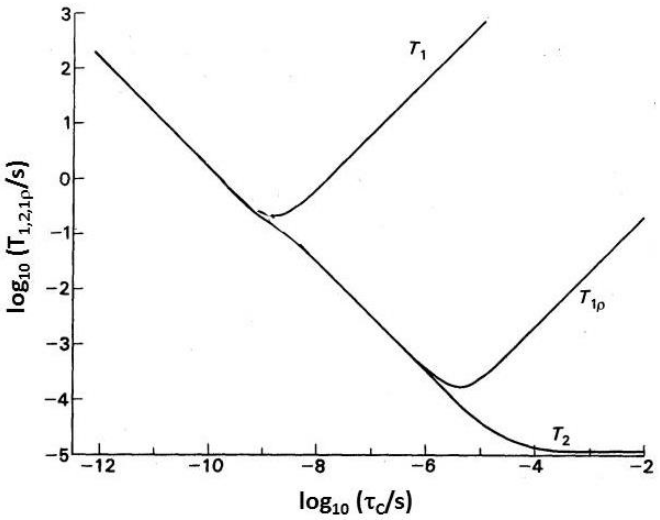

Figure S5: NMR relaxation correlation plot, displaying the dependence of T_{1H}, $T_{1\rho H}$ and T_{2H} on the correlation time of molecular tumbling (τ_C).[4] A shorter correlation time implies quicker tumbling (e.g. faster segmental polymer chain motions). In the case of T_{1H} and $T_{1\rho H}$, the relaxation time goes through a minimum at $\tau_c \sim 1/\omega_0$ (with ω_0 the Larmor frequency) and $\tau_c \sim 1/\omega_1$ (with ω_1 the spin-lock frequency), respectively. Further increase of the correlation time (rigidity) beyond this minimum will result in an increase of the relaxation time. As $PC_{71}BM$ crystals are highly rigid and ordered, the τ_C will be situated at the right side of the $T_{1\rho H}$ (and T_{1H}) minimum. The long T_{1H} and $T_{1\rho H}$ fractions are thus attributed to the crystalline phase. For the pure polymers, the flexible alkyl side chains exhibit a very short τ_C due to a high degree of rotational freedom around the carbon-carbon σ bonds, situating them at the left side of the minima. This rationalizes that the proton fraction with the long $T_{1\rho H}$ decay time in the polymer samples can be assigned to the protons of the flexible alkyl side chains.

10. References

[1] J.F. Bard, L. R., Electrochemical methods: fundamentals and applications, 2nd ed., Wiley: New York2001.
[2] S. Trasatti, The absolute electrode potential: an explanatory note (Recommendations 1986), Pure Appl. Chem., 58 (1986) 955-966.
[3] C. Cabanetos, A. El Labban, J.A. Bartelt, J.D. Douglas, W.R. Mateker, J.M. Frechet, M.D. McGehee, P.M. Beaujuge, Linear side chains in benzo[1,2-b:4,5-b']dithiophene-thieno[3,4-c]pyrrole-4,6-dione polymers direct self-assembly and solar cell performance, J Am Chem Soc, 135 (2013) 4656-4659.
[4] R.K. Harris, Nuclear magnetic resonance spectroscopy: a physicochemical view, Longman Scientific & Technical1986.